

Conf-9510158-1

UCRL-JC-120677
PREPRINT

Detailed and Global Chemical Kinetics Model for Hydrogen

**N. M. Marinov
C. K. Westbrook
W. J. Pitz**

**This paper was prepared for submittal to the
8th International Symposium
on Transport Properties
October 1995
San Francisco, CA**

March 1995

**This is a preprint of a paper intended for publication in a journal or proceedings. Since
changes may be made before publication, this preprint is made available with the
understanding that it will not be cited or reproduced without the permission of the
author.**



DISCLAIMER

This document was prepared as an account of work sponsored by an agency of the United States Government. Neither the United States Government nor the University of California nor any of their employees, makes any warranty, express or implied, or assumes any legal liability or responsibility for the accuracy, completeness, or usefulness of any information, apparatus, product, or process disclosed, or represents that its use would not infringe privately owned rights. Reference herein to any specific commercial product, process, or service by trade name, trademark, manufacturer, or otherwise, does not necessarily constitute or imply its endorsement, recommendation, or favoring by the United States Government or the University of California. The views and opinions of authors expressed herein do not necessarily state or reflect those of the United States Government or the University of California, and shall not be used for advertising or product endorsement purposes.

DISCLAIMER

**Portions of this document may be illegible
in electronic image products. Images are
produced from the best available original
document.**

Detailed and Global Chemical Kinetics Model For Hydrogen

N.M. Marinov, C.K. Westbrook and W.J. Pitz

Lawrence Livermore National Laboratory

P.O. Box 808, L-298, Livermore, CA. 94551

USA

Abstract

Detailed and global chemical kinetic computations for hydrogen-air mixtures have been performed to describe flame propagation, flame structure and ignition phenomena. Simulations of laminar flame speeds, flame compositions and shock tube ignition delay times have been successfully performed. Sensitivity analysis was applied to determine the governing rate-controlling reactions for the experimental data sets examined. In the flame propagation and structure studies, the reactions, $\text{OH} + \text{H}_2 = \text{H}_2\text{O} + \text{H}$, $\text{O} + \text{H}_2 = \text{OH} + \text{H}$ and $\text{O} + \text{OH} = \text{O}_2 + \text{H}$ were the most important in flames. The shock tube ignition delay time study indicated the $\text{H} + \text{O}_2 + \text{M} = \text{HO}_2 + \text{M}$ ($\text{M} = \text{N}_2, \text{H}_2$) and $\text{O} + \text{OH} = \text{O}_2 + \text{H}$ reactions controlled ignition.

A global rate expression for a one step overall reaction was developed and validated against experimental hydrogen-air laminar flame speed data. The global reaction expression was determined to be

$$k_{\text{global}} = 1.8 \times 10^{13} \exp(-17614K/T) [\text{H}_2]^{1.0} [\text{O}_2]^{0.5}$$

for the single step reaction $\text{H}_2 + 1/2\text{O}_2 = \text{H}_2\text{O}$.

MASTER

Introduction

The public concern for improved urban air quality, finite fossil fuel resources, and global warming trends support the need for a clean burning alternative fuel. Hydrogen is an attractive alternative fuel, because it does not produce CO₂ greenhouse gas, offers the potential of reduced NO_X pollutant emissions, can enhance fuel economy when used in hydrocarbon mixtures and is virtually limitless in supply.

Hydrogen as a fuel is unique because of its simple oxidation kinetics, very fast mass diffusivity and low molecular weight. Interestingly, all chemical reactions that consume molecular hydrogen in the H₂ - O₂ system produce atomic hydrogen which is an extremely reactive and diffusive species. The hydrogen atom is the most important radical needed for flame propagation and ignition in virtually all combustion systems. However, the transport properties of this species have a high degree of uncertainty relative to other species and, therefore, the accuracy of computations involving H₂ as a fuel is problematic.

The purpose of this paper is to describe the reaction kinetics for hydrogen combustion which is suitable for describing flame propagation, flame composition measurements and ignition delay times. A detailed reaction mechanism was developed and validated against laminar flame speeds for a wide range of hydrogen - air stoichiometries, flame structure measurements of a low pressure rich H₂ / O₂ / Ar laminar flame and shock

tube ignition delay times near the second explosion limit. In addition, a one-step global rate expression for the single step reaction $H_2 + 1/2 O_2 = H_2O$ was developed and validated against laminar flame speed data.

Reaction Mechanism

The detailed reaction mechanism used in this study is given in Table 1. The reverse rate constants are calculated from the forward rate constants through the equilibrium rate constants derived from the CHEMKIN thermochemical database [11]. The chemical kinetic reaction rates used for the $H_2 - O_2$ chain branching / propagating submechanism (reactions 1-4) are well known and are considered to be accurate to within a factor of 1.5 for the 300K - 2500K temperature range. The $H_2 - O_2$ dissociation / recombination reactions have been critically reviewed by Dixon - Lewis [5] and, Tsang and Hampson [6]. Reactions 5, 6, and 8 are accurate to within a factor of 2, and reaction 7 is accurate to a factor of 10. Greater uncertainty in the kinetics exists for those reactions which form or consume HO_2 radicals and H_2O_2 . A detailed review of the chemical kinetics literature was performed to critically evaluate these reactions.

In figures 1 and 2, the $H + O_2 + M = HO_2 + M$ (M = any third body) reaction was evaluated over the 300K - 2500K temperature range. The $H + O_2 + M = HO_2 + M$ (M = Ar) reaction was primarily fit to the measurements of Wong and Davis [12], Carleton et al. [13], Hsu et al. [14], Pirraglia et al. [15], Gay and Pratt [16], and Pamidimukkala and Skinner [17].

The $\text{H} + \text{O}_2 + \text{H}_2 = \text{HO}_2 + \text{H}_2$ reaction was fitted to the data of Nielsen et al. [18] and Kochubei and Moin [19]. The $\text{H} + \text{O}_2 + \text{N}_2 = \text{HO}_2 + \text{N}_2$ reaction was fitted primarily to the studies of Hsu et al. [14], Slack [20] and Peeters et al. [21]. These resulting fits are within the uncertainty factor of three prescribed to the Baulch recommended rates involving these reactions for the 300K - 2000K temperature range [9]. The kinetic rate applied to the $\text{H} + \text{O}_2 + \text{H}_2\text{O} = \text{HO}_2 + \text{H}_2\text{O}$ reaction was derived from using the fitted rate of reaction 9a and then using the Hsu et al. [14] relation of $k_{\text{H}_2\text{O}} / k_{\text{He}} = 23.9 (T / 300)^{-1.18}$ (assuming $\text{M} = \text{He} = \text{Ar}$) for the 298K - 635K temperature range. Discrepancies in the literature values for third body efficiencies of H_2O at temperatures greater than 1000K makes the kinetic rate for reaction 9d suspect to error. However, the fitted kinetic rate for this reaction agrees, to within a factor of two, with the Baulch recommendation in the 1000K - 2000K temperature range.

The kinetic rate for $\text{H} + \text{HO}_2 = \text{H}_2 + \text{O}_2$ was fitted to the low temperature measurements of Keyser [22], intermediate temperature measurements of Baldwin and Walker [23], and to the reverse rate of this reaction at high temperatures as determined by Koike [24]. The $\text{OH} + \text{OH} (+\text{M}) = \text{H}_2\text{O}_2 (+\text{M})$ reaction was fitted by using a complex set of rate parameters in the Troe fall-off formulation [25]. This complex fit was validated against the experimental measurements of Zellner et al. [26], Troe [27,28], Brouwer et al. [29] and Basevich et al. [30]. The $\text{H}_2\text{O}_2 + \text{H} = \text{HO}_2 + \text{H}_2$ reaction was fitted to a T^2 expression (analogous to the H-atom abstraction reaction $\text{H}_2\text{O}_2 + \text{O} = \text{OH} + \text{HO}_2$) by using the data of Albers et al. [31], and Baldwin and Walker [23]. The $\text{H}_2\text{O}_2 + \text{OH} = \text{H}_2\text{O} + \text{HO}_2$ reaction was primarily

fitted to the measurements of Hippler and Troe [32], Baldwin et al. [33,34], Kurylo et al. [35], and Keyser [36].

Reaction Kinetics of H₂ - Air Laminar Flame Speeds

Recent experimental data [37 - 44] for the laminar flame speed (S_L) of atmospheric H₂ / Air mixtures have been compiled and are shown in figures 3 and 4. In figure 3, a ~70cm/sec variation in S_L around Φ (H₂ fuel to air equivalence ratio) of 1.4 is exhibited, while in figure 4, considerable scatter by as much as ~60cm/sec in S_L is found for lean hydrogen mixtures. The observed discrepancies in the H₂ / Air laminar flame speeds is due to aerodynamic flame strain (or stretch). Aerodynamic flame strain is caused by preferential mass and thermal diffusion, and flow divergence [45,46]. Experimental data uncorrected for these effects represent a strain dependent flame speed and *not* the true (strain-free) laminar flame speed (S_L). This study has modeled the flame strain corrected experimental data for H₂ / Air laminar flame speeds at one atmosphere. A one-dimensional, premixed, laminar flame code (PREMIX) [47] was used to perform the computations with the detailed H₂ / O₂ / N₂ / Ar mechanism and transport [48]. All calculations were performed using multi-component mass transport and thermal diffusion.

Numerical calculations show good agreement with the experimental laminar flame speed data for the full range of hydrogen-air stoichiometries (figure 3). A laminar flame speed maximum of 300cm/sec at an equivalence ratio of 1.6 and atmospheric pressure was calculated, also in

agreement with the measured data. In addition, computations performed at equivalence ratios of 0.30, 1.0 and 4.0 predict flame speed values of 5.9cm/sec, 210cm/sec, and 144cm/sec, all of which are good.

A sensitivity analysis of the important chemical reactions which influence the mass burning rate (or the laminar flame speed) was performed at equivalence ratios of 0.6, 1.0 and 1.4. The results are shown in figure 5. The normalized sensitivity coefficient was calculated through the expression,

$$(A_i / m_L) (\Delta m_L / \Delta A_i) \quad (1)$$

where A_i is the pre-exponential factor of the i^{th} reaction rate expression and m_L is mass burning rate (where $m_L = \rho_u S_L$, ρ_u is the unburned gas density). The results show that the dominant reactions promoting flame propagation are the chain reactions $\text{OH} + \text{H}_2 = \text{H}_2\text{O} + \text{H}$, $\text{O} + \text{OH} = \text{O}_2 + \text{H}$ and $\text{O} + \text{H}_2 = \text{OH} + \text{H}$, and the HO_2 consumption reaction $\text{HO}_2 + \text{H} = \text{OH} + \text{O}_2$. The dominant reaction retarding flame propagation is $\text{HO}_2 + \text{H} = \text{H}_2 + \text{O}_2$.

As the H_2 / Air stoichiometry goes from rich to lean, the laminar flame speed becomes more sensitive to $\text{OH} + \text{O} = \text{O}_2 + \text{H}$ and reactions involving the HO_2 radical. The forward reaction in $\text{H} + \text{O}_2 = \text{OH} + \text{O}$ is endothermic and therefore its chemical kinetic rate is especially sensitive to temperature changes as hydrogen mixtures become leaner. The HO_2 radical, primarily produced by $\text{H} + \text{O}_2 + \text{M} = \text{HO}_2 + \text{M}$ (M = any third body), competes with the $\text{H} + \text{O}_2 = \text{O} + \text{OH}$ reaction for the H-atom. At ultra-lean conditions (Φ less than 0.5), reactions involving the HO_2 radical become very important.

For example, the $\text{H} + \text{O}_2 + \text{M} = \text{HO}_2 + \text{M}$ reaction competes with $\text{H} + \text{O}_2 = \text{OH} + \text{O}$ for H-atom thereby strongly influencing the OH radical pool for the main H_2 consumption reaction $\text{OH} + \text{H}_2 = \text{H}_2\text{O} + \text{H}$, and/or the $\text{H} + \text{HO}_2 = \text{OH} + \text{OH}$ reaction can convert an unreactive HO_2 radical to a reactive OH thereby promoting the chain propagating reaction $\text{OH} + \text{H}_2 = \text{H}_2\text{O} + \text{H}$. As indicated in figure 5, the highest sensitivity coefficient calculated was for the $\text{OH} + \text{H}_2 = \text{H}_2\text{O} + \text{H}$ reaction at $\Phi = 0.6$ and this reaction is most important for flame propagation at lean conditions.

While detailed reaction mechanisms provide insight into flame structure and reactivity of gas mixtures, there is a great need for one-step global kinetics for use in complex fluid mechanics codes that utilize two- to three-dimensional geometry. The computational effort of using detailed kinetics in such models is not practical. Therefore, a one-step overall reaction was developed and validated against laminar flame speed data. The global reaction study made use of the HCT code [49] for the laminar flame speed computations. The global reaction rate parameters were varied in order to obtain good agreement between computed and experimentally observed flame speeds. The global rate expression for hydrogen-air laminar flame speeds was determined to be

$$k_{\text{global}} = 1.8 \times 10^{13} \exp(-17614K/T) [\text{H}_2]^{1.0} [\text{O}_2]^{0.5} \quad (2)$$

for the single step reaction $\text{H}_2 + 1/2 \text{O}_2 = \text{H}_2\text{O}$.

Figures 3 and 4 shows the comparison of the experimentally measured laminar flame speeds with the computed ones using the global reaction

model. The predicted flame speed well represented the experimental data for only the 0.55 - 1.1 equivalence ratio range. Predictions by the global reaction model were considered poor outside this equivalence ratio range. The poor prediction is attributed to chemical and thermal structure changes in the flame as the stoichiometry varies which could not be properly accounted for in the global reaction model.

Reaction Kinetics of a Low Pressure Rich Hydrogen-Oxygen-Argon Flame

While comparison with laminar flame speed data is a valuable test of a detailed reaction mechanism, a more demanding validation method is to compare experimental flame structure data with numerical computations. The structure of a low pressure rich H₂ /O₂ /Ar laminar flame investigated by Vandooren and Bian [50] was used to validate the chemical kinetic model. These experimental measurements were performed at a pressure of 35.5 torr (0.047 atm) which differed from the laminar flame speed measurements performed at 1 atmosphere. This large difference in pressure allowed the two body reactions in the detailed mechanism to be tested at these conditions.

The experimental data were obtained using a premixed, flat flame burner. The composition of the incoming reactants was 39.7% H₂, 10.3% O₂ and 50% Ar (equivalence ratio of 1.91) and had an in flow velocity of 131 cm/sec. Flame structure measurements were performed by molecular beam sampling with a mass spectrometer. Measurement errors of the stable compounds (H₂, O₂, H₂O) were estimated to be ~2% and for

radicals (OH, O-atom, H-atom) ~10%. Computations were performed using the PREMIX code with the measured temperature profile as given in the reference [50].

Figure 6 shows the comparison of the experimental mole fraction profiles of the stable species with the computed ones. The predicted molecular hydrogen profile agreed very well with the measured profile. About 40% of the initial hydrogen was predicted to remain in the burnt gases, in good agreement with the experimental results, as supported by the model prediction. The predicted profile for the molecular oxygen mole fraction agreed well with the data. However, there exists some discrepancy between the model and the experimental data for O₂ in the preheating zone of the flame close to the burner. The experimental and computed maximum concentrations of water were identical and both profiles exhibited the same gradient of H₂O formation. If the experimental profile for water was shifted by approximately 0.5mm towards the burner surface, better agreement would result. Reaction flux analysis was applied to this flame and determined that H₂ was destroyed a factor of two faster by reaction 2 than reaction 4. The O₂ was primarily removed by reaction 1 with secondary reactions 9a and 9b playing a minor role. Water was formed exclusively from reaction 2.

Figure 7 shows the comparison of the experimental mole fraction profiles of the radical species with the computed ones. For all three radical species, the model predictions are somewhat higher than the measured values. The computed profile for the hydroxyl radicals exhibited the same

profile behavior as the experimental measurements, however the detailed kinetic model overestimated the hydroxyl concentration by a factor of 1.75 - 2.0 at the peak OH level and in the post-flame zone. The location of the predicted maximum for the O-atom corresponds well with experimental data. The model overpredicted the O-atom concentration by a factor of 1.7 - 2.0 in the flame and post-flame zones. The model overpredicted the H-atom concentration by ~60% at the peak H-atom level and predicted to within a factor of two the H-atom concentration in the post-flame zone. Model predictions for the radical species were worse in the preheat zone of the flame with the H-atom overpredicted by a factor of five. The HO₂ concentration was not measured in this flame but the model predicted a peak HO₂ mole fraction of 7.5E-6 at ~0.05mm downstream from the burner surface. Reaction flux analysis was applied to this flame and determined that the OH radical was primarily produced by reactions 1 and 4 and destroyed by reaction 2, while in the preheat zone OH was also formed by reaction 11. The O-atom was produced by reaction 1 and destroyed by reaction 4. The H-atom was produced a factor of two faster by reaction 2 than reaction 4 , while H-atom was removed by reaction 1. The HO₂ radical was formed a factor of two faster by reaction 9b than reaction 9a, while reaction 11 consumed HO₂ a factor of three faster than reaction 10.

These numerical computations indicate that overpredicting the radical concentrations by as much as a factor of two does not have an adverse impact on predicting stable species concentrations or possibly the laminar flame speeds. However, we can not provide an explanation to justify our finding.

Reaction Kinetics of Shock Tube Ignition Delay Times

The shock tube experimental data of Slack [20] were used to test the present H₂ / O₂ / N₂ / Ar mechanism for ignition delay near the second explosion limit. Stoichiometric hydrogen-air mixtures were heated by reflected shock waves at 2 atmospheres and for the 980K - 1176K reflected shock temperature range. Numerical simulations were performed with the SENKIN code [51] assuming that the gas dynamics behaves in an adiabatic constant volume process.

In figure 8, the ignition delay data of Slack are compared to the numerical computations. For temperatures below ~1025K, the experimental ignition delay times become significantly longer as the experimental conditions approach the second explosion limit (classically defined as $2 k_{rev,1} / k_{9a,b,c,d} = [M]$). The detailed chemical model predicted the same behavior. For temperatures above ~1100K, the ignition delay time is shorter and is predicted correctly by the model.

A sensitivity analysis of the important chemical reactions which influence the ignition delay time was conducted at temperatures of 1000K and 1111K. The results are shown in Table 2. In the sensitivity analysis, the pre-exponential factor, A, for each reaction was perturbed upward by a factor of 2 while maintaining the same equilibrium rate constant. The ignition delay was then computed at the same experimental conditions as the baseline case. The sensitivity coefficient values shown in Table 2 are represented by the expression:

$$\ln(t_{ign}(\text{perturbed}) / t_{ign}(\text{baseline}))$$

(3)

A positive coefficient denotes an increase in the ignition delay time and a negative coefficient denotes a decrease in ignition delay. An inspection of Table 2 shows that the chain branching reaction 1 and the chain terminating reactions 9a, 9b and 9c [52] are, as expected, of greatest importance. An increase of a factor of two in the chemical kinetic rate of reactions 9b and 9c resulted in a factor of ~20 increase to the ignition delay time at 1000K. The uncertainty factor associated with these reactions is a factor of three for the 300K - 2000K temperature range [9]. The perturbed change in the kinetic rate for $H + O_2 + M = HO_2 + M$ ($M = N_2, H_2$) is well within the uncertainty factor established for this reaction and demonstrates the need for further kinetic rate studies involving this important chain terminating process. The $O + OH = O_2 + H$ reaction showed a factor of ~5 decrease in the ignition delay time at 1000K and its kinetic rate is relatively well-known. For temperatures at 1111K, reaction 1 exhibited the highest sensitivity to the ignition delay time with reactions 9b and 9c showing a minor influence at this higher temperature.

Although the ignition delay time is very sensitive to reactions 1, 9a, 9b, and 9c, this study also examined the sensitivity of the ignition delay times to other reaction rates. Chain reactions such as $O + H_2 = OH + H$ and $H + HO_2 = OH + OH$ reduce ignition delay by producing reactive radicals OH and H. The $H + HO_2 = H_2 + O_2$ reaction is chain terminating at 1000K as it consumes a reactive H-atom plus an unreactive HO₂ radical to make

stable products. However, at 1111K, the reverse rate of this reaction begins to become important as the reactants H₂ and O₂ produce H and HO₂ radicals at these very short residence times.

Summary

Detailed and global chemical kinetics for hydrogen-air mixtures have been validated against data derived from flame propagation, flame structure and shock tube ignition delay time studies. The chemical kinetic mechanism for the detailed reaction model was critically reviewed and well-simulated the experimental measurements. A global rate expression validated against hydrogen-air laminar flame speeds was developed for the single step reaction H₂ + 1/2 O₂ = H₂O.

Acknowledgement

This work was carried out under the auspices of the U.S. Department of Energy by the Lawrence Livermore National Laboratory under contract No. W-7405-ENG-48.

References

1. Masten, D.A.; Hanson, R.K.; and Bowman, C.T.: *J. Phys. Chem.*, **94**, 7119, 1990.
2. Michael, J.V.: *Prog. Energy Comb. Sci.*, **18**, 327, 1992.
3. Wooldridge, M.S.; Hanson, R.K., and Bowman, C.T.: *Int. J. Chem. Kin.*, **26**, 389, 1994.
4. Sutherland, J.W.; Patterson, P.M.; and Klemm, R.B.: *J. Phys. Chem.*, **94**, 2471, 1990.
5. Dixon-Lewis, G.: *Archivum Combustionis*, **4**, 279, 1984.
6. Tsang, W.; and Hampson, R.F.: *J. Phys. Chem. Ref. Data*, **15**, 1095, 1986.
7. Cobos, C.J.; Hippler, H.; and Troe, J.: *J. Phys. Chem.*, **89**, 342, 1985.
8. Warnatz, J.: *In Combustion Chemistry*; (Gardiner, W.C., Ed.); Chapter 5, Springer-Verlag, 1984.
9. Baulch, D.L.; Cobos, C.J.; Cox, R.A.; Esser, C.; Frank, P.; Just, Th.; Kerr, J.A.; Pilling, M.J.; Troe, J.; Walker, R.W.; and Warnatz, J.: *J. Phys. Chem. Ref. Data*, **21**, 411, 1992.
10. Hippler, H.; Troe, J.; and Willner, J.: *J. Chem. Phys.*, **93**, 1755, 1990.
11. Kee, R.J.; Rupley, F.M.; and Miller, J.A.: Sandia National Laboratory, Albuquerque, N.M., SAND87-8215B, 1987.
12. Wong, W.; and Davis, D.D.: *Int. J. Chem. Kin.*, **6**, 401, 1974.
13. Carleton, K.L.; Kessler, W.J.; and Marinelli, W.J.: *J. Phys. Chem.*, **93**, 1018, 1989.
14. Hsu, K.J.; Anderson, S.M.; Durant, J.L.; and Kaufman, F.: *J. Phys. Chem.*, **93**, 282, 1989.

15. Pirraglia, A.N.; Michael, J.V.; Sutherland, J.W.; and Klemm, R.B.;
J. Phys. Chem., **93**, 282, 1989.
16. Gay, A.; and Pratt, N.H.: *Proceedings of Eighth (international) Shock Tube Symposium*, Chapman and Hall, London, 39, 1971.
17. Pamidimukkala, K.M.; and Skinner, G.B.: *Thirteenth (International) Symposium of Shock Tubes and Waves*, SUNY Press: Albany, N.Y., 585, 1981.
18. Nielsen, O.J.; Sillesen, A.; Luther, K.; and Troe, J.:
J. Phys. Chem., **86**, 2929, 1982.
19. Kochubei, V.F.; and Moin, F.B.: Ukr. Khim. Zh., **39**, 888, 1973.
20. Slack, M.W.: Comb. Flame, **28**, 241, 1977.
21. Peeters, J.; and Mahnen, G.: Fourteenth Symposium (International) on Combustion, 133, The Combustion Institute, 1973.
22. Keyser, L.F.: J. Phys. Chem. , **90**, 2994, 1986.
23. Baldwin, R.R.; and Walker, R.W.: Seventeenth Symposium (International) on Combustion, 525, The Combustion Institute, 1979.
24. Koike, T.: Bull. Chem. Soc. Jpn., **62**, 2480, 1989.
25. Gilbert, R.G.; Luther, K.; and Troe, J.: Ber. Bunsenges. Phys. Chem., **87**, 169, 1983.
26. Zellner, R.; Ewig, F.; Paschke, R.; and Wagner, H.:
J. Phys. Chem., **92**, 4184, 1988.
27. Troe, J.: Ber. Bunsenges. Phys. Chem., **73**, 946, 1969.
28. Troe, J.: J. Chem. Soc. Faraday Trans., **90**, 2303, 1994.
29. Brouwer, L.; Cobos, C.J.; Troe, J.; Dubai, H.R.; and Crim, L.L.:
J. Chem. Phys., **86**, 6171, 1987.

30. Basevich, V. Y.; Kogarko, S.M.; and Berezin, O.Y.:
Izv. Akad. Nauk SSR, 9, 1986, 1979.

31. Albers, E.A.; Hoyerman, H.; Wagner, H.G.; and Wolfrum, J.:
Thirteenth Symposium (International) on Combustion, 81, The
Combustion Institute, 1971.

32. Hippler, J.; and Troe, J.: Chem. Phys. Lett., 192, 333, 1992.

33. Baldwin, R.R.; and Mayor, L.: Trans. Faraday Soc., 57, 1578, 1960.

34. Baldwin, R.R.; and Bratten, D.: *Eighth Symposium (International) on
Combustion*, 110, The Combustion Institute, 1962.

35. Kurylo, M.; Murphy, J.; Haller, G.; and Curnett, K.: Int. J. Chem. Kin.,
14, 1149, 1982.

36. Keyser, L.: J. Phys. Chem., 84, 1659, 1980.

37. Koroll, G.W.; Kumar, R.K.; and Bowles, E.M.: Comb. Flame,
94, 330, 1993.

38. Vagelopoulos, C.; Egolfopoulos, F.N.; and Law, C.K.: *Twenty-Fifth
Symposium (International) on Combustion*, The Combustion Institute,
1994.

39. Berman, M.: Sandia National Laboratory, Albuquerque, N.M.,
SAND84-0689, 1984.

40. Takahashi, F.; Mizomoto, M.; and Ikai, S.: Alternative Energy Sources III
(T. Nejat Veziroglu, Ed.), 447, Vol. 5 Nuclear Energy / Synthetic Fuels,
1983.

41. Wu, C.K.; and Law, C.K.: *Twentieth Symposium (International) on
Combustion*, 1941, The Combustion Institute, 1984.

42. Dowdy, D.R.; Smith, D.B.; Taylor, S.C.; and Williams, A.: *Twenty-Third Symposium (International) on Combustion*, 325, The Combustion Institute, 1990.
43. Egolfopoulos, F.N.; and Law, C.K.: *Twenty-Third Symposium (International) on Combustion*, 333, The Combustion Institute, 1990.
44. Iijima, T.; and Takeno, T.: *Comb. Flame*, **65**, 35, 1986.
45. Matalon, M.; and Matkowsky, B.J.: *J. Fluid. Mech.*, **124**, 239, 1982.
46. Law, C.K.: *Twenty-Second Symposium (International) on Combustion*, 1381, The Combustion Institute, 1988.
47. Kee, R.J.; Grcar, J.F.; Smooke, M.D.; and Miller, J.A.: Sandia National Laboratory, Albuquerque, N.M., SAND85-8240, 1985.
48. Kee, R.J.: Dixon-Lewis, G.; Warnatz, J.; Coltrin, M.E.; and Miller, J.A.: Sandia National Laboratory, Albuquerque, N.M., SAND86-8246, 1986.
49. Lund, C.M.: Lawrence Livermore National Laboratory Report UCRL-52504, 1978.
50. Vandooren, J.; and Bian, J.: *Twenty-Third Symposium (International) on Combustion*, 341, The Combustion Institute, 1990.
51. Lutz, A.E.; Kee, R.J.; and Miller, J.A.: Sandia National Laboratory, Albuquerque, N.M.; SAND87-8248, 1988.
52. The HO₂ radical produced from reaction 9 exhibits very low reactivity and, therefore, reaction 9 behaves more as a chain terminating reaction than a chain propagating reaction.
53. Clyne, M.A.A.; and Thrush, B.A.: *Proc. R. Soc. London, Ser. A*, **A275**, 559, 1963.

Table 1
H₂ / O₂ / N₂ / Ar Reaction Mechanism

Units are cm³ - mole - sec - kcal - K

$$k = A T^n \exp(-E_a/RT)$$

No.	Reaction	ΔH^0_{298K}	A _{fwd}	n _{fwd}	E _{a,fwd}	Reference
<i>H₂-O₂ Chain Reactions</i>						
1.	O + OH = O ₂ + H	-16.77	2.02E+14	-0.40	0.0	Masten et al. [1]
2.	OH + H ₂ = H + H ₂ O	-15.01	2.14E+08	1.52	3.449	Michael et al. [2]
3.	OH + OH = O + H ₂ O	-16.88	3.57E+04	2.40	-2.112	Wooldridge et al. [3]
4.	O + H ₂ = OH + H	1.85	5.06E+04	2.67	6.290	Sutherland et al. [4]
<i>H₂-O₂ Dissociation/Recombination Reactions</i>						
5a.	H + H + M = H ₂ + M ^{a,b}	-104.2	1.00E+18	-1.00	0.000	Dixon-Lewis [5]
5b.	H + H + H ₂ = H ₂ + H ₂	-104.2	9.27E+16	-0.60	0.000	Dixon-Lewis [5]
5c.	H + H + H ₂ O = H ₂ + H ₂ O	-104.2	6.00E+19	-1.25	0.000	Dixon-Lewis [5]
6.	O + O + M = O ₂ + M	-119.1	1.89E+13	0.00	-1.788	Tsang et al. [6]
7.	O + H + M = OH + M	-102.3	4.71E+18	-1.00	0.000	Tsang et al. [6]
8.	H + OH + M = H ₂ O + M	-119.2	2.21E+22	-1.25	0.000	Tsang et al. [6]
<i>Formation and Consumption of HO₂</i>						
9a.	H + O ₂ + M = HO ₂ + M ^c	-49.6	$k_0 = 1.05E+19$	$T^{-1.257}$		Compiled Fit [d,e]
			$k_\infty = 4.517E+13$			Cobos et al. [7]
9b.	H + O ₂ + H ₂ = HO ₂ + H ₂	-49.6	$k_0 = 1.52E+19$	$T^{-1.133}$		Compiled Fit [d,f]
			$k_\infty = 4.517E+13$			Cobos et al. [7]
9c.	H + O ₂ + N ₂ = HO ₂ + N ₂	-49.6	$k_0 = 2.031E+20$	$T^{-1.590}$		Compiled Fit [d,f]
			$k_\infty = 4.517E+13$			Cobos et al. [7]
9d.	H + O ₂ + H ₂ O = HO ₂ + H ₂ O	-49.6	$k_0 = 2.10E+23$	$T^{-2.437}$		Compiled Fit [d]
			$k_\infty = 4.517E+13$			Cobos et al. [7]
10.	HO ₂ + H = H ₂ + O ₂	-54.6	8.45E+11	0.65	1.241	Compiled Fit [d]
11.	HO ₂ + H = OH + OH	-35.97	1.50E+14	0.00	1.000	Warnatz [8]
12.	HO ₂ + H = O + H ₂ O	-52.85	3.01E+13	0.00	1.721	Baulch et al. [9]
13.	HO ₂ + O = OH + O ₂	-51.73	3.25E+13	0.00	0.000	Baulch et al. [9]
14.	HO ₂ + OH = H ₂ O + O ₂	-69.61	2.89E+13	0.00	-0.497	Baulch et al. [9]
<i>Formation and Consumption of H₂O₂</i>						
15.	HO ₂ + HO ₂ = H ₂ O ₂ + O ₂	-37.53	$k = 4.20E+14 \exp(-11.98/RT) + 1.30E+11 \exp(+1.629/RT)$			Hippler et al. [10]
16.	OH + OH + M = H ₂ O ₂ + M ^g	-51.14	$k_\infty = 1.24E+14$	$T^{-0.37}$		Compiled Fit [d]
			$k_0 = 3.041E+30 T^{-4.63} \exp(-2.049/RT)$			
	Troe Parameters / $a=0.47$ $T^{***}=100$. $T^*=2000$. $T^{**}=1.E+15$ /					
17.	H ₂ O ₂ + H = H ₂ O + OH	-68.05	3.07E+13	0.00	4.217	Baulch et al. [9]
18.	H ₂ O ₂ + H = HO ₂ + H ₂	-17.07	1.98E+06	2.00	2.435	Compiled Fit [d]
19.	H ₂ O ₂ + O = OH + HO ₂	-15.20	9.55E+06	2.00	3.970	Tsang et al. [6]
20.	H ₂ O ₂ + OH = H ₂ O + HO ₂	-32.08	2.40E+00	4.042	-2.162	Compiled Fit [d]

a) $[M] = \sum \varepsilon_i [c_i]$ where ε_i represents the chaperon efficiency and $[c_i]$ represents the concentration of the i^{th} species. b) $\varepsilon_{H2} = 0.0$; $\varepsilon_{H2O} = 0.0$ and all other species have efficiencies equal to unity.

c) $\varepsilon_{H2} = 0.0$; $\varepsilon_{H2O} = 0.0$; $\varepsilon_{N2} = 0.0$ and all other species have efficiencies equal to unity.

d) See text for description of the reaction rate expression fit. e) See Figure 1 f) See Figure 2

g) Troe fall-off reaction form: $F_{\text{cent}} = (1 - a) \exp(-T/T^{***}) + a \exp(-T/T^*) + \exp(-T^{**}/T)$

Table 2
Sensitivity Analysis of Computed
Ignition Delay Times

No.	Reaction	In ($\tau_{ign}(\text{perturbed}) / \tau_{ign}(\text{baseline})$)	
		1000K	1111K
9b.	$\text{H} + \text{O}_2 + \text{H}_2 = \text{HO}_2 + \text{H}_2$	3.03	0.18
9c.	$\text{H} + \text{O}_2 + \text{N}_2 = \text{HO}_2 + \text{N}_2$	3.03	0.18
1.	$\text{O} + \text{OH} = \text{O}_2 + \text{H}$	-1.67	-0.61
9a.	$\text{H} + \text{O}_2 + \text{M} = \text{HO}_2 + \text{M}$	0.48	0.04
11.	$\text{HO}_2 + \text{H} = \text{OH} + \text{OH}$	-0.13	-0.02
4.	$\text{O} + \text{H}_2 = \text{OH} + \text{H}$	-0.09	-0.08
10.	$\text{HO}_2 + \text{H} = \text{H}_2 + \text{O}_2$	0.08	-0.02
8.	$\text{H}_2\text{O}_2 + \text{H} = \text{HO}_2 + \text{H}_2$	-0.03	0.00
2.	$\text{OH} + \text{H}_2 = \text{H} + \text{H}_2\text{O}$	-0.02	-0.02
12.	$\text{HO}_2 + \text{H} = \text{O} + \text{H}_2\text{O}$	-0.02	-0.01
13.	$\text{HO}_2 + \text{O} = \text{O}_2 + \text{OH}$	0.01	0.00

Figure Captions

FIGURE 1. An Arrhenius plot for $H + O_2 + M = HO_2 + M$ reaction, $M = Ar$. Data from references [12 - 17] were used to generate the curve fit.

FIGURE 2. Arrhenius plots for $H + O_2 + H_2 = HO_2 + H_2$ and $H + O_2 + N_2 = HO_2 + N_2$. Data from references [18,19] were used to generate the curve fit to $H + O_2 + H_2 = HO_2 + H_2$. Data from references [14,20, 21] were used to generate the curve fit to $H + O_2 + N_2 = HO_2 + N_2$.

FIGURE 3. Hydrogen -air laminar flame speeds at 1 atmosphere and $T_U = 298K$ as a function of equivalence ratio. Equivalence ratio range is 0.15 to 6.0. Comparison between experimental data [37 - 44] (symbols) and computations (detailed model - solid line, global reaction model - dashed line).

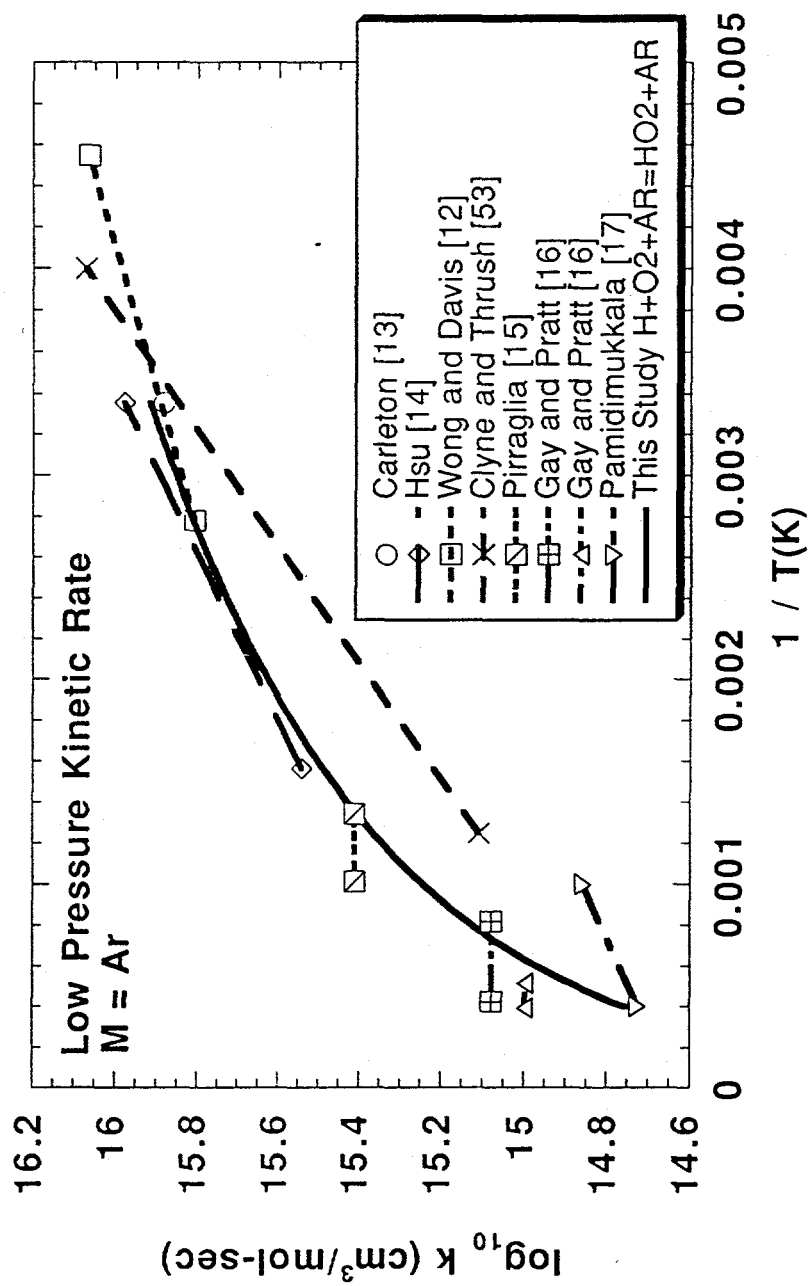
FIGURE 4. Hydrogen -air laminar flame speeds at 1 atmosphere and $T_U = 298K$ as a function of equivalence ratio. Equivalence ratio range is 0.15 to 0.80. Comparison between experimental data [37 - 44] (symbols) and computations (detailed model - solid line, global reaction model - dashed line).

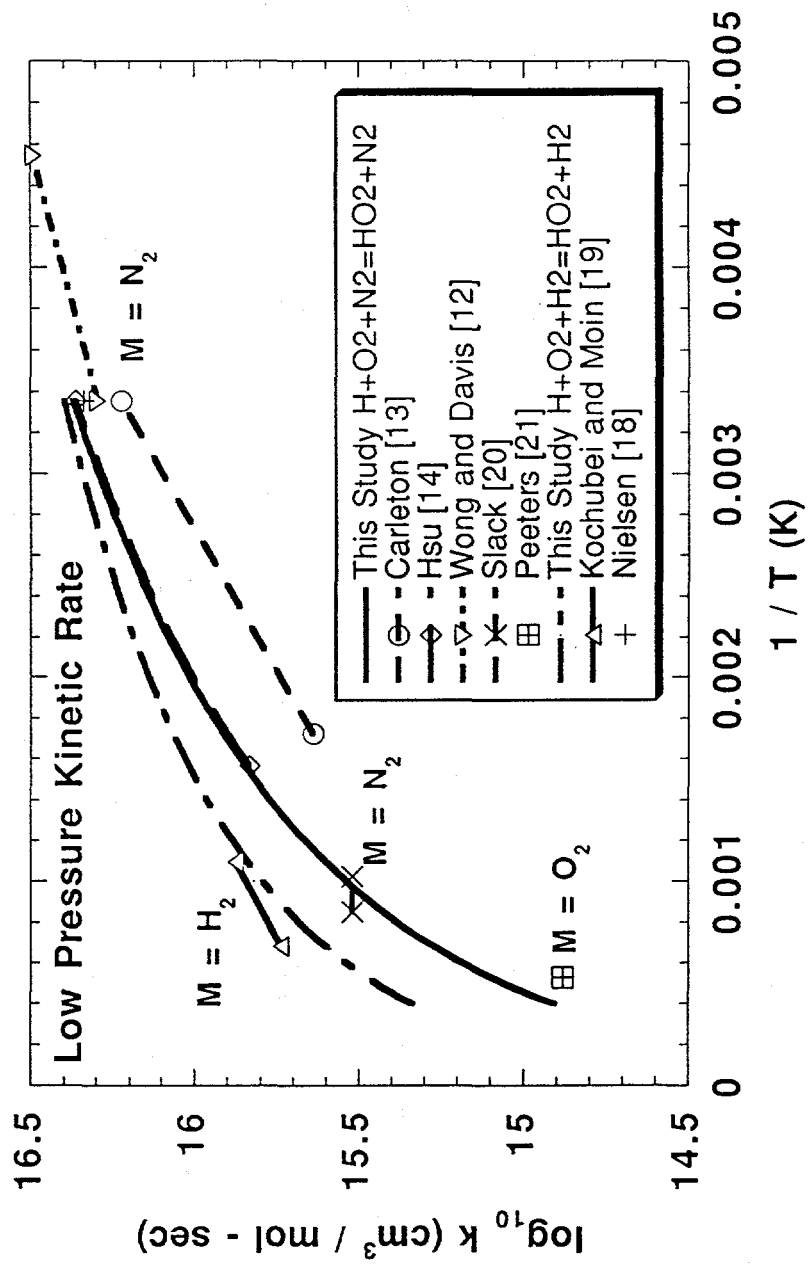
FIGURE 5. Sensitivity Analysis of hydrogen - air laminar flame speeds at 1 atmosphere and $T_U = 298K$. Normalized first order sensitivity coefficients given by $(A_i / m_L) (\Delta m_L / \Delta A_i)$ where A_i is the pre-exponential factor to the rate constant of the i -th reaction and m_L is mass burning rate ($m_L = \rho_U S_L$).

FIGURE 6. Rich Hydrogen-Oxygen-Argon Flame [50] of the inlet composition 39.7% H_2 , 10.3% O_2 , and 50.0% Ar ($\Phi = 1.91$ equivalence ratio), operating pressure 35.5torr and initial velocity of 131cm/sec. Comparison between computations (lines) and experimental data for H_2 , O_2 and H_2O (symbols).

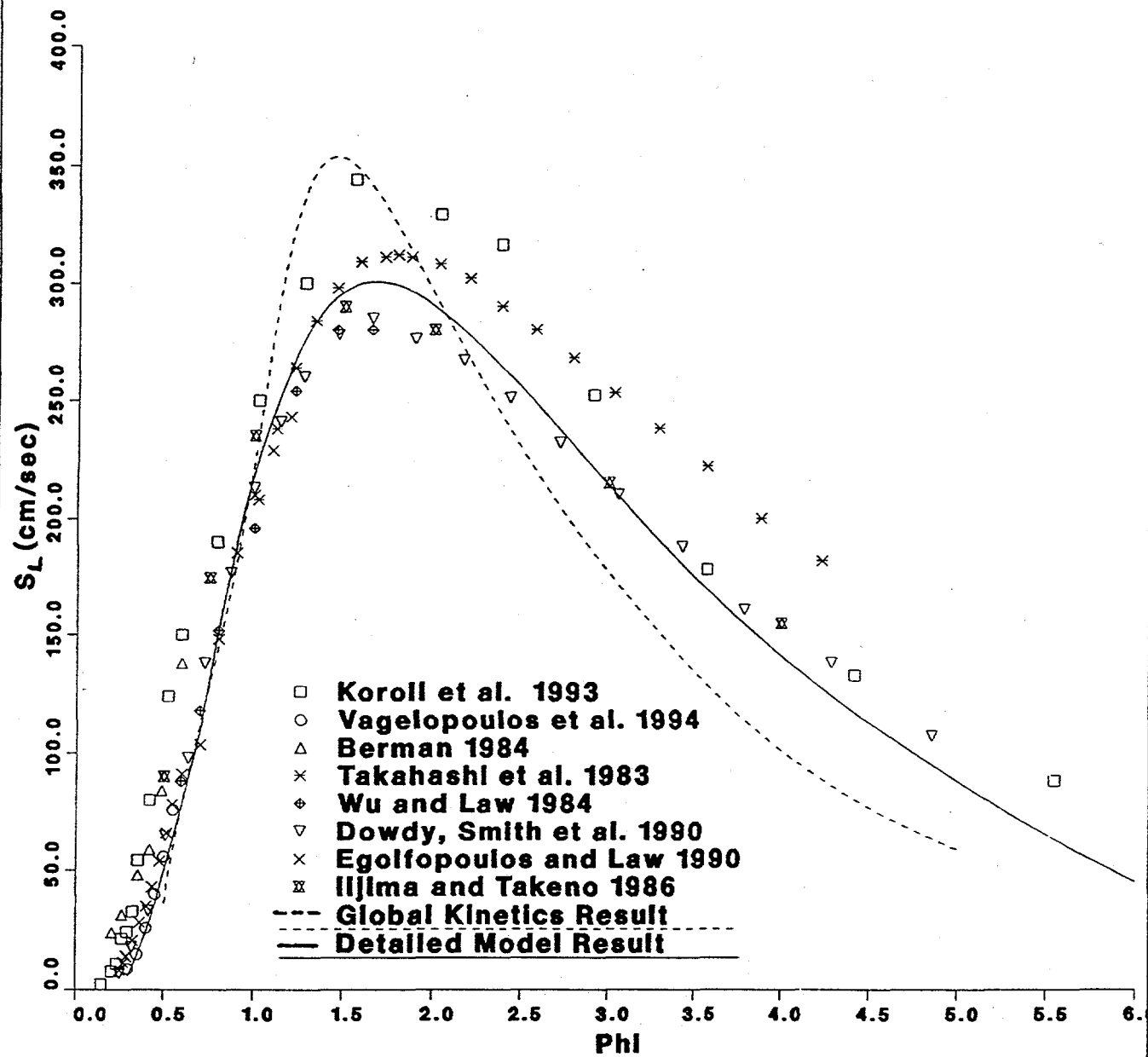
FIGURE 7. Rich Hydrogen-Oxygen-Argon Flame [50] of the inlet composition 39.7% H_2 , 10.3% O_2 , and 50.0% Ar ($\Phi = 1.91$ equivalence ratio), operating pressure 35.5torr and initial velocity of 131cm/sec. Comparison between computations (lines) and experimental data for OH , O-atom and H-atom (symbols).

FIGURE 8. Ignition delay times of stoichiometric hydrogen - air at 2 atmospheres. Comparison between experimental data [20] (circles) and computations (lines).

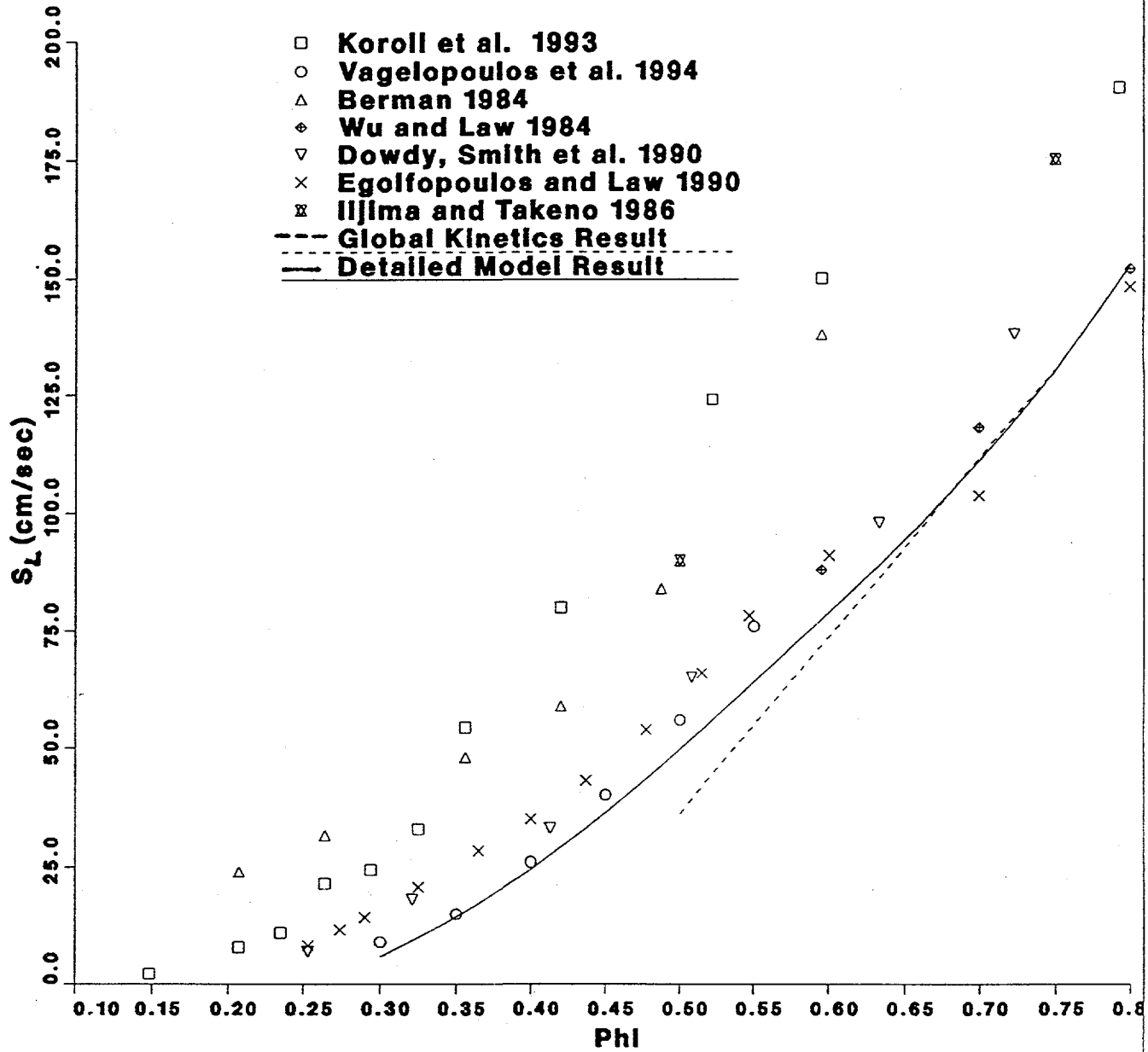




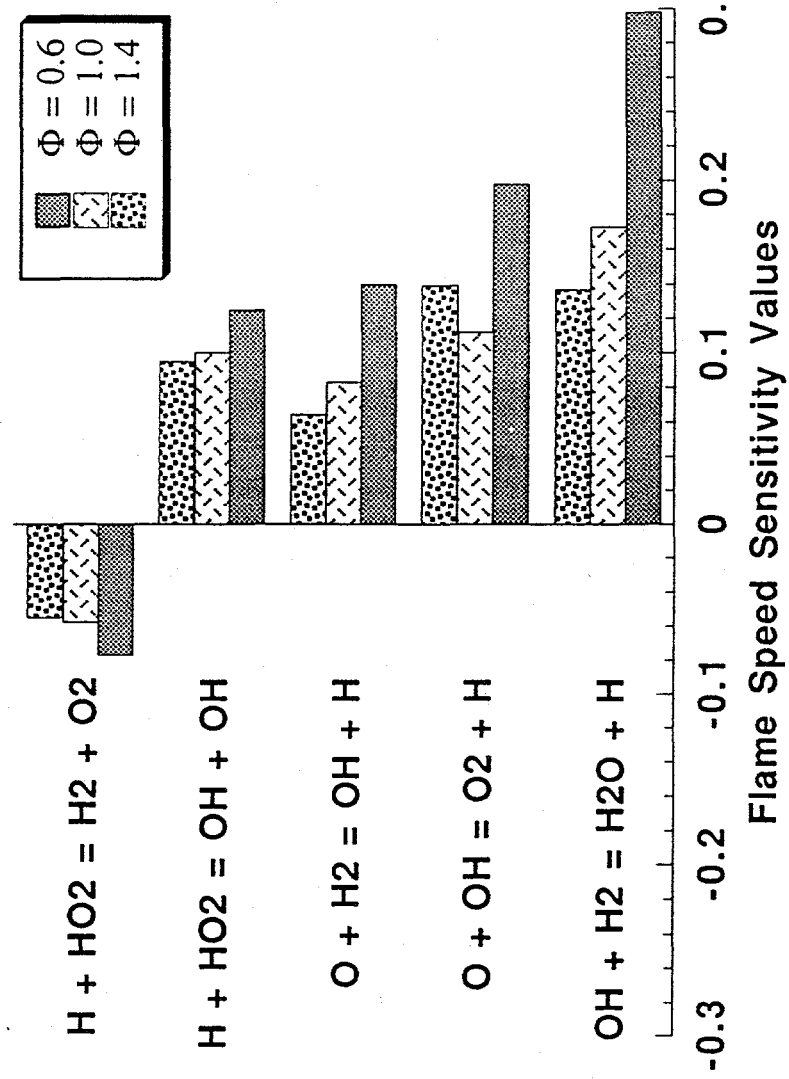
H2 - Air Laminar Flame Speed

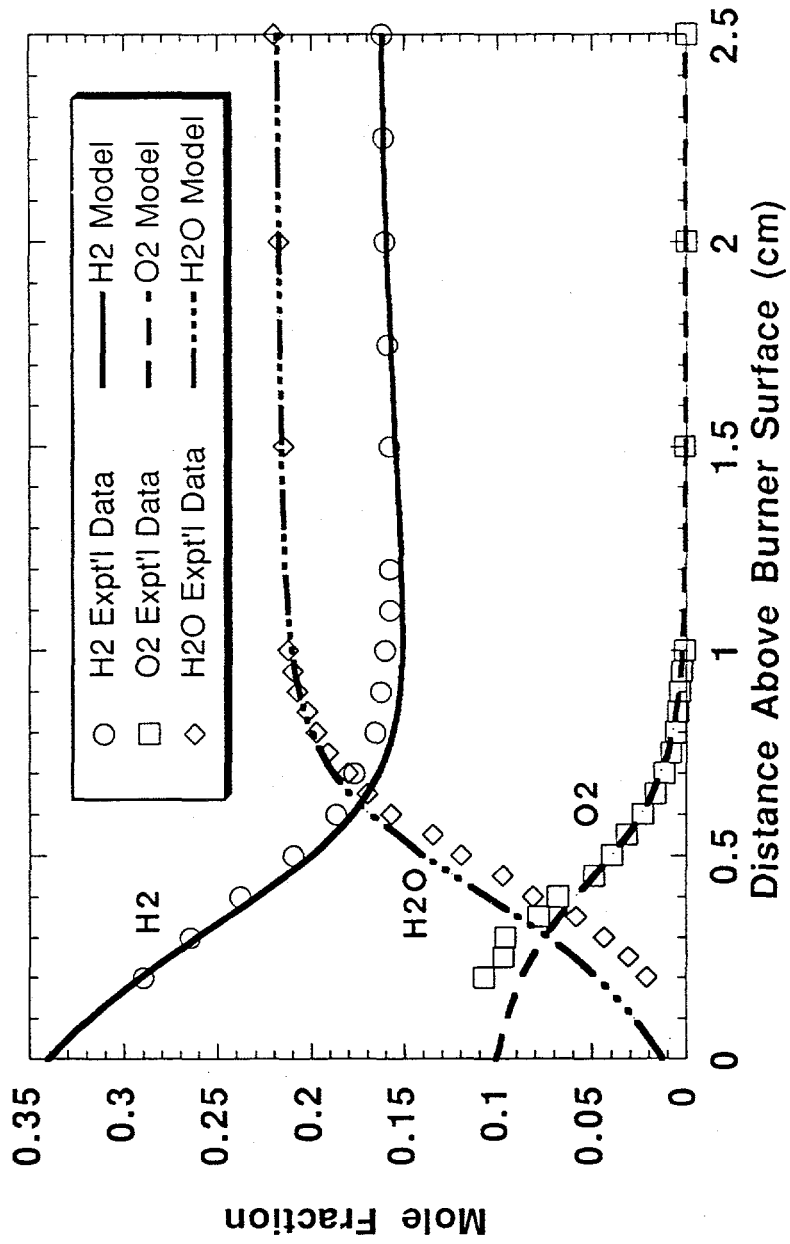


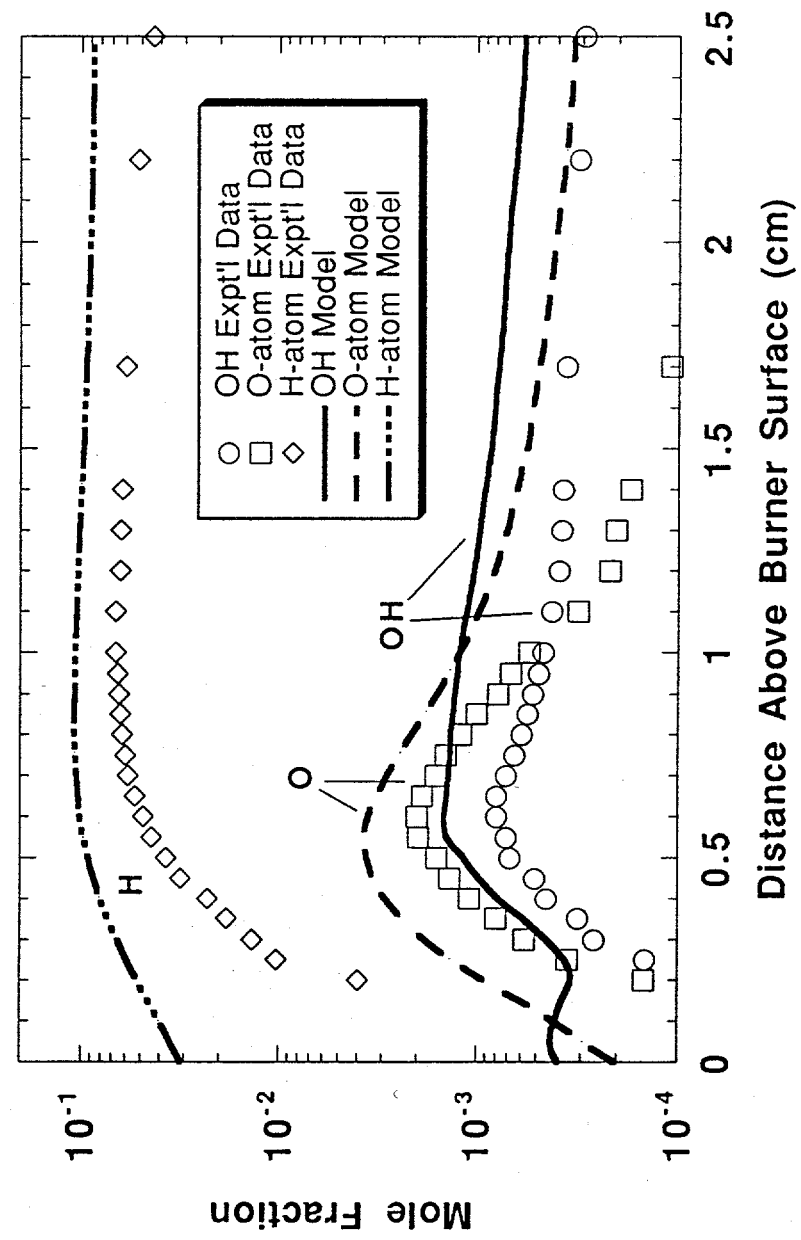
H2 - Air Laminar Flame Speed

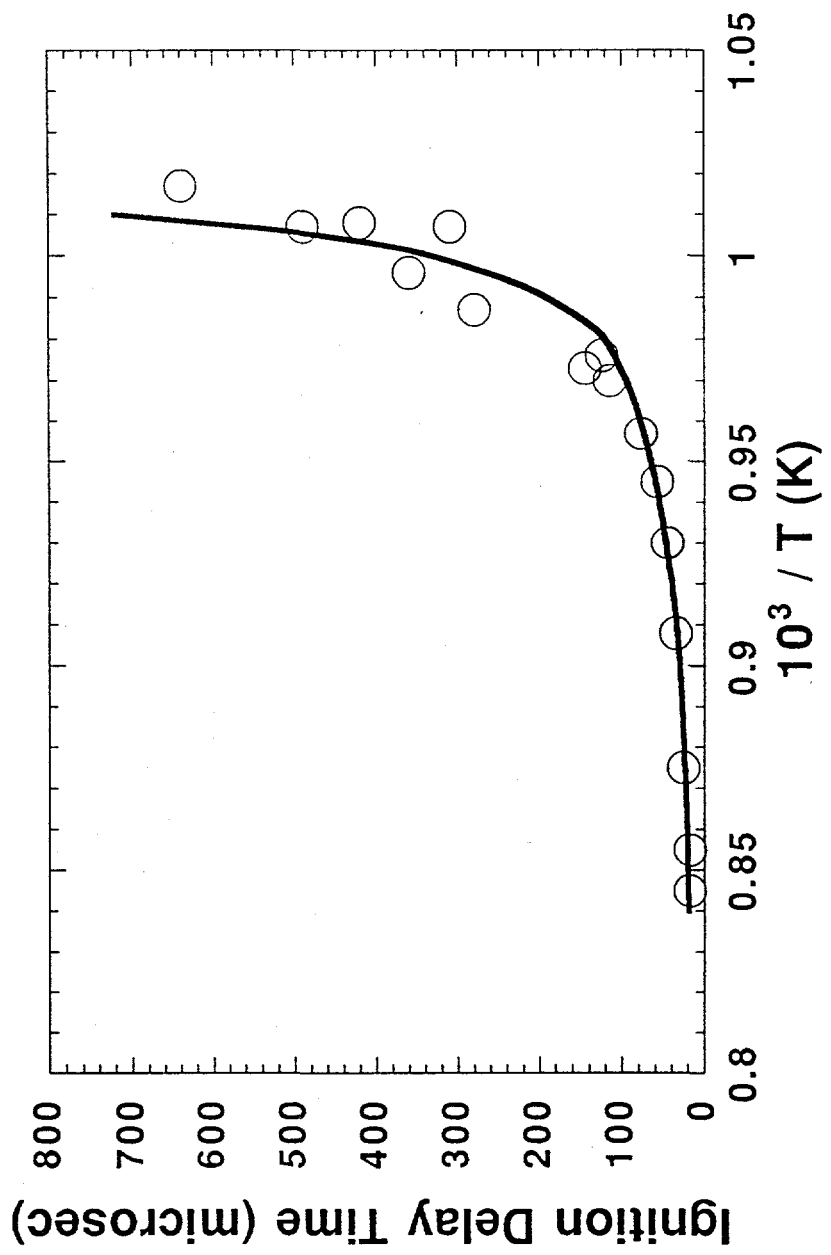


Laminar Flame Speed Sensitivity Analysis for H₂ - Air









Chemical Kinetic and Fluid Mechanical Modeling of Hydrogen Combustion

LLNL has completed a rather extensive review of the chemical kinetic reaction mechanisms for hydrogen oxidation, particularly in flames. An improved reaction mechanism has been developed which has been found to reproduce experimental laminar flame propagation and structure measurements accurately. In addition, we have also provided a simplified, one-step reaction mechanism, over a wide range of hydrogen/air equivalence ratios. This simplified mechanism can be used in multidimensional CFD models such as the LANL KIVA codes where computational speed is required or the additional accuracy of the detailed reaction scheme is not required. We are currently in the process of testing both this simplified mechanism as well as the detailed reaction mechanism for hydrogen oxidation in a code based on the KIVA model, and we will report in the future on the results of this study, emphasizing both the relative computational costs and accuracy of the results.

The one-dimensional study of hydrogen oxidation in flames has been submitted to the Eighth International Symposium on Transport Processes, and the text of this paper is attached to this report. The detailed kinetic and simplified reaction mechanisms are provided explicitly in the paper, along with discussions of the sources of the reaction rates and the sensitivity of the computed results to rate data. Additional copies of this paper are available from the authors.